

Frustrated ferromagnetic spin- $\frac{1}{2}$ chain in a magnetic field: The phase diagram and thermodynamic properties

F. Heidrich-Meisner,^{1,2} A. Honecker,^{3,4} and T. Vekua^{5,6}

¹*Materials Science and Technology Division, Oak Ridge National Laboratory, Oak Ridge, Tennessee 37831, USA*

²*Department of Physics and Astronomy, University of Tennessee, Knoxville, Tennessee 37996, USA*

³*Institut für Theoretische Physik, Universität Göttingen, 37077 Göttingen, Germany*

⁴*Institut für Theoretische Physik, Technische Universität Braunschweig, 38106 Braunschweig, Germany*

⁵*Laboratoire de Physique Théorique, Université Louis Pasteur, 67084 Strasbourg Cedex, France*

⁶*Andronikashvili Institute of Physics, Tamarashvili 6, 0177 Tbilisi, Georgia*

(Received 18 May 2006; revised manuscript received 1 July 2006; published 27 July 2006)

The frustrated ferromagnetic spin- $1/2$ Heisenberg chain is studied by means of a low-energy field theory as well as the density-matrix renormalization group and exact diagonalization methods. First, we study the ground-state phase diagram in a magnetic field and find an “even-odd” (EO) phase characterized by bound pairs of magnons in the region of two weakly coupled antiferromagnetic chains. A jump in the magnetization curves signals a first-order transition at the boundary of the EO phase, but otherwise the curves are smooth. Second, we discuss thermodynamic properties at zero field, where we confirm a double-peak structure in the specific heat for moderate frustrating next-nearest-neighbor interactions.

DOI: 10.1103/PhysRevB.74.020403

PACS number(s): 75.10.Pq, 75.40.Cx, 75.30.Kz, 75.40.Mg

The physics of frustrated quantum spin systems is currently attracting large interest as exotic quantum phases may emerge.¹ Prominent examples are quantum-disordered ground states with different patterns of broken translational symmetry and quantum chiral phases (see, e.g., Ref. 2). In addition, some frustrated systems have a large number of low-lying excitations, leading to unusual features in thermodynamic quantities.

In one dimension, the paradigmatic model is the frustrated spin- $1/2$ chain

$$H = \sum_l [J_1 \vec{s}_l \cdot \vec{s}_{l+1} + J_2 \vec{s}_l \cdot \vec{s}_{l+2}] - h \sum_l s_l^z. \quad (1)$$

\vec{s}_l are spin $s=1/2$ operators at site l , while h denotes a magnetic field.

Much is known about the ground-state properties and the magnetic phase diagram of the frustrated antiferromagnetic (AFM) chain with $J_1, J_2 > 0$.² We highlight the appearance of a plateau in the magnetization curve at magnetization $M=1/3$ and the existence of an “even-odd” (EO) region at small J_1 with spins flipping in pairs in a magnetic field h .³

Relatively little attention has been paid to frustrated ferromagnetic (FM) chains, i.e., $J_1 < 0$ and $J_2 > 0$, until the recent discovery of materials described by parameters with this combination of signs. We mention in particular $\text{Rb}_2\text{Cu}_2\text{Mo}_3\text{O}_{12}$ which is believed to be described by $J_1 \approx -3J_2$,⁴ and LiCuVO_4 which lies in a different parameter regime with $J_1 \approx -0.3J_2$.⁵ In both cases, the saturation field h_{sat} is within experimental reach. A recent transfer-matrix renormalization group (TMRG) study⁶ of the thermodynamics of Eq. (1) was motivated by the experimental results for $\text{Rb}_2\text{Cu}_2\text{Mo}_3\text{O}_{12}$.

In this paper we study the zero-temperature phase diagram in a magnetic field and the thermodynamics of Eq. (1) at zero field. The former is obtained by a combination of a low-energy field theory and the density-matrix renormaliza-

tion group (DMRG) method,⁷ while the latter is computed by exact diagonalization (ED). We develop a minimal effective field theory description for the region of small J_1 and $h < h_{\text{sat}}$ and predict the existence of an EO phase. Note that at $J_1 = -4J_2$, the system undergoes a transition to a FM ground state.⁸ The field theory predictions are verified by our DMRG results. Further, our ground-state phase diagram differs qualitatively from recent mean-field predictions.⁹ In our study of thermodynamic properties,¹⁰ we focus on the example of $J_1 = -3J_2$ and present data for system sizes up to $N=24$ sites. The specific heat of LiCuVO_4 will be discussed elsewhere.¹¹

First we discuss an effective field theory describing the long-wavelength fluctuations of Eq. (1) in the limit of strong next-nearest-neighbor interactions $J_2 \gg |J_1|$.

Just below the saturation field, the problem can be mapped onto a dilute gas of bosons.¹² This mapping, which is asymptotically exact in the subspace of two magnons, shows that magnons bind in pairs for any $J_1 < 0$. Although the two-magnon state is not always realized as a ground state in a magnetic field,¹³ Chubukov¹² found that in this subspace and for $-0.38J_1 < J_2$, the ground-state momentum is commensurate while for $-0.25J_1 < J_2 < -0.38J_1$, it becomes incommensurate. Based on the discontinuous nature of the change of momentum for the lowest two-magnon bound state, Chubukov further predicted a first-order phase transition between a chiral and a dimerized nematiclike phase.

Apart from the issue of the two-magnon states being realized as ground states, the mapping onto a dilute gas of bosons is controlled just near the saturation field $h \approx h_{\text{sat}}$. We apply a complementary bosonization procedure which is controlled for $h < h_{\text{sat}}$ and confirm that the hallmark property of the commensurate region—pair binding of magnons—is universal and extends well below the saturation field. A good starting point is the limit of $J_2 \gg |J_1|$ and a finite magnetic field $h \neq 0$.¹³ In this limit, the system may be viewed as two AFM chains subject to an external magnetic field and weakly

coupled by the FM zigzag interaction J_1 . It is well known that the low-energy effective field theory for a single isolated spin-1/2 chain ($J_1=0$) in a uniform magnetic field is the Tomonaga-Luttinger liquid¹⁴

$$\mathcal{H} = \frac{v}{2} \int dx \left(\frac{1}{K} (\partial_x \phi)^2 + K (\partial_x \theta)^2 \right). \quad (2)$$

Above we have introduced a compactified scalar bosonic field ϕ and its dual counterpart θ , with $[\phi(x), \theta(y)] = i\Theta(y-x)$, where $\Theta(x)$ is the Heaviside function.

The Luttinger liquid (LL) parameter $K(h)$ and spin-wave velocity $v(h)$ can be related to microscopic parameters of the lattice model J_2 and h using the Bethe-ansatz solution of the Heisenberg chain in a magnetic field.^{15,16} We recall here that $K(h)$ increases monotonically with the magnetic field from $K(h=0)=1/2$ to the universal free-fermion value $K=1$ for h approaching the saturation field $h_{\text{sat}}=2J_2$. The Fermi wave vector $k_F = \frac{\pi}{2}(1-M)$ is determined by the magnetization M . Note that we normalize the magnetization to $M=1$ at saturation, i.e., $M=2S^z/N$ with $S^z = \sum_i s_i^z$.

Now we perturbatively add the interchain coupling term to two chains, each of which is described by an effective Hamiltonian of the form Eq. (2) and fields ϕ_i , $i=1,2$. For convenience, we transform to the symmetric and antisymmetric combinations $\phi_{\pm} = (\phi_1 \pm \phi_2)/\sqrt{2}$ and $\theta_{\pm} = (\theta_1 \pm \theta_2)/\sqrt{2}$. In this basis and apart from terms \mathcal{H}_0^{\pm} of the form (2), the effective Hamiltonian describing low-energy properties of Eq. (1) contains a single relevant coupling with the coupling $g_1 \propto J_1 \ll v$:

$$\mathcal{H}_{\text{eff}} = \mathcal{H}_0^+ + \mathcal{H}_0^- + g_1 \int dx \cos(k_F + \sqrt{8\pi}\phi_-), \quad (3)$$

and the renormalized LL parameter

$$K_- = K(h) \{1 + J_1 K(h) / [\pi v(h)]\}. \quad (4)$$

The Hamiltonian (3) yields the minimal effective low-energy field theory describing the region $J_2 \gg |J_1|$ of the frustrated FM spin-1/2 chain for $M \neq 0$. The relevant interaction term $\cos \sqrt{8\pi}\phi_-$ opens a gap in the ϕ_- sector. Since $s_{i+1}^z - s_i^z \sim \partial_x \phi_-$, relative fluctuations of the two chains are locked, leading to pair binding of magnons. These bound pairs of magnons themselves are gapless, since $s_{i+1}^z + s_i^z \sim \partial_x \phi_+$. This phase was observed for an AFM J_1 in Ref. 3 and dubbed the EO phase.

In addition, we confirm this picture numerically. The simplest possible lattice model that is described by a low-energy effective Hamiltonian of type (3) is a spin ladder with a dominant biquadratic leg-leg interaction.¹⁷ We compute the magnetization curve with DMRG (results not presented here) and verify that only even magnon sectors are realized as ground states for all fields $h > 0$.

Equation (4) shows that the LL parameter K_- decreases with an increasing absolute value $|J_1|$ of the FM interchain coupling, in contrast to an AFM coupling. However, the bosonization procedure becomes inapplicable once K_- vanishes. This signals an instability of the EO phase when increasing $|J_1|$. Moreover, we conclude that for FM J_1 , the EO

phase extends up to the saturation field h_{sat} (since $K_- < 1$ for $J_1 < 0$ such that there is always a relevant coupling in the antisymmetric sector), in contrast to the AFM case.

To check this scenario and determine the phase boundaries, we perform DMRG calculations for up to 156 sites imposing open boundary conditions. The finite-system algorithm⁷ is used and we keep up to 350 states. DMRG gives direct access to the ground-state energies $E_0(S^z, h=0)$ at zero magnetic field in subspaces labeled by S^z . After shifting the ground-state energies $E_0(S^z, h=0)$ by a Zeeman term through $E_0(S^z, h) = E_0(S^z, h=0) - hS^z$, it is straightforward to construct the magnetization curve.

We start the discussion from the limit $|J_1| \leq J_2$. The magnetization curves for $J_1 = -J_2$ are shown in Fig. 1(a). In particular, we verify the pair binding of magnons predicted above: in a wide parameter range in the magnetic phase diagram (h vs J_1), the magnetization changes in steps of $\Delta S^z = 2$. This can be observed even on systems as small as $N=24$, while for an AFM interchain coupling $J_1 > 0$, the formation of bound states was only reported for long chains.³

From the inset of Fig. 1(a), which shows data for $J_1 = -2.5J_2$, we conclude that a second phase emerges at lower fields, signaled by a change of the magnetization steps from $\Delta S^z = 1$ to 2 at $h = h_{\text{jump}}$. This transition is first order.

In contrast to the frustrated antiferromagnetic chain,³ no indications of an $M=1/3$ plateau are found. We find that the width of the 1/3 plateau as seen in finite systems scales to zero with $1/N$.

The magnetization curve exhibits further features when J_1 approaches the transition to the FM regime, occurring at $J_1 = -4J_2$. The main observations from Fig. 1(b), which shows $M(h)$ for $J_1 = -3J_2$, and additional data not displayed in the figures, are as follows. Below saturation, the steps in $M(h)$ are of size $\Delta S^z = 3$ [see, e.g., the case of $J_1 = -3J_2$ in Fig. 1(b)]. Upon decreasing $J_1 \rightarrow -4J_2$, the magnetization curve becomes very steep below saturation and the steps of ΔS^z may even be larger than 3. For instance, we find steps of $\Delta S^z = 4$ for $J_1 = -3.75$ and $N=60$ below saturation. Nevertheless, the asymptotic behavior of $M(h)$ close to the saturation field for $J_1 = -3J_2$ [see Fig. 1(b)] is consistent with a standard square-root singularity in $M(h)$ (see Ref. 13 and references therein).

Our main findings for the magnetic phase diagram are displayed in Fig. 1(c), where h is normalized by h_{sat} .^{12,18} The largest part of the phase diagram belongs to the EO phase, while the transition to the region with $\Delta S^z = 1$ is first order. The position of this line, i.e., h_{jump} (dotted, with stars) is consistent with results of Ref. 12 in the high-field limit, but the transition takes place at lower h/h_{sat} for smaller $|J_1|$. For larger J_1 and fields $h > h_t$, a third region emerges, characterized by $\Delta S^z = 3$. Just as for AFM J_1 ,¹⁹ one may speculate about chiral order in some of these regions as well as additional phases, but substantially larger system sizes might be needed to fully reveal the nature of this part of the phase diagram.

Next we discuss thermodynamic properties concentrating on $h=0$. We perform full diagonalizations to obtain all eigenvalues and then use spectral representations to compute thermodynamic quantities, as described in some detail for the

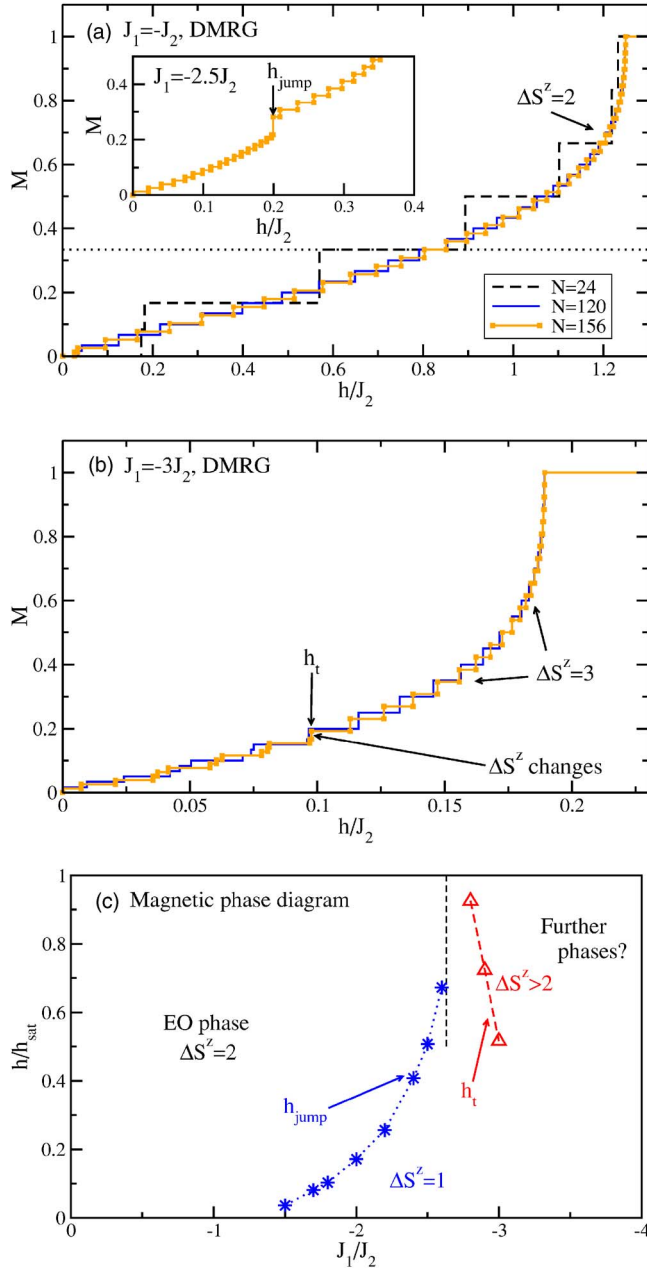


FIG. 1. (Color online) (a) Main panel (inset): Magnetization curve $M(h)$ for $J_1 = -J_2$ ($J_1 = -2.5J_2$). The horizontal dotted line marks $M = 1/3$. (b) $M(h)$ for $J_1 = -3J_2$. (c) Magnetic phase diagram of the frustrated FM chain. The dotted line (with stars) marks the first-order transition between the EO phase and the $\Delta S^z = 1$ region, while the line $h = h_t$ (dashed, triangles) separates the $\Delta S^z = 1$ region from the $\Delta S^z \geq 3$ part. Uncertainties of the transition lines, e.g., due to finite-size effects, should not exceed the size of the symbols. The fields h_{jump} and h_t were extracted from $N = 156$ sites (stars) and $N = 120$ sites (triangles), respectively. The dashed, vertical line is the result of Ref. 12 ($J_2 \approx 0.38J_1$).

entropy in Ref. 20. In order to render the Hamiltonian (1) translationally invariant, we now impose periodic boundary conditions. After symmetry reduction, the biggest matrices to be diagonalized for $N = 24$ are of complex dimension 81 752. In such high dimensions, we use a custom shared-memory

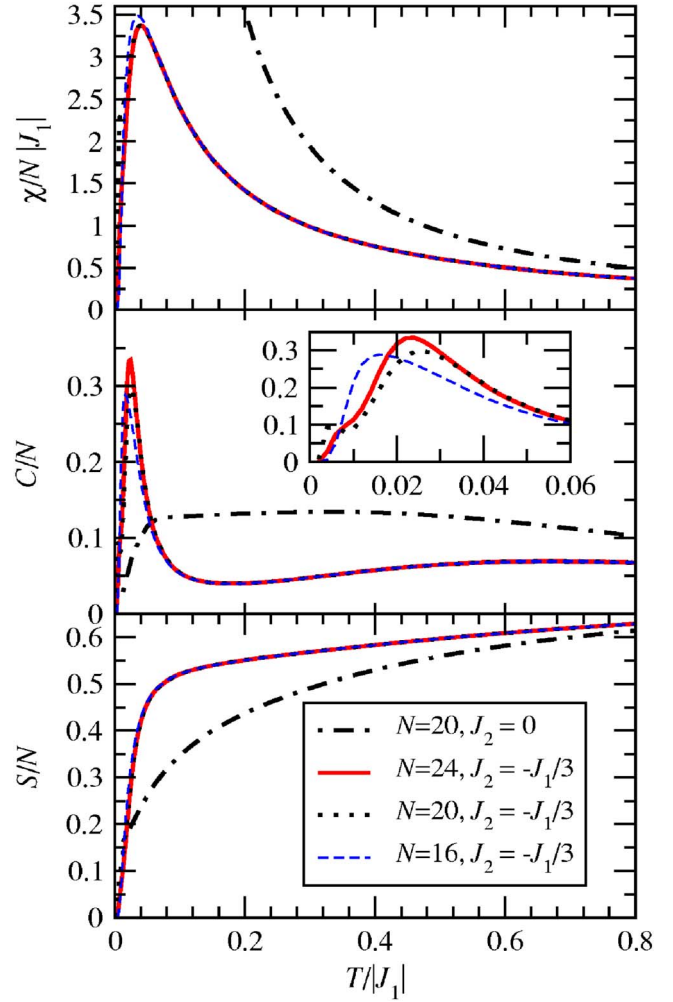


FIG. 2. (Color online) Magnetic susceptibility (top panel), specific heat (middle panel), and entropy per site (bottom panel) for $N = 16, 20$, and 24 at $J_1 = -3J_2$, $h = 0$ in comparison to a FM chain with $J_2 = 0$ and $N = 20$. Middle panel, inset: specific heat at low temperatures for $J_1 = -3J_2$.

parallelized Householder algorithm, while standard library routines are used in lower dimensions.

Figure 2 shows results at $J_2 = -J_1/3$ and $h = 0$ for rings with $N = 16, 20$, and 24 . This ratio of exchange constants is close to values suggested for $\text{Rb}_2\text{Cu}_2\text{Mo}_3\text{O}_{12}$,⁴ and the phase diagram in a magnetic field promises interesting properties in this parameter regime. Both the magnetic susceptibility χ and the specific heat C have a maximum at low temperatures, namely, for $N = 24$ at $T \approx 0.04|J_1|$ in the case of χ and $T \approx 0.023|J_1|$ in the case of C . While these low-temperature maxima are affected by finite-size effects, the dependence on N is negligible at higher temperatures. The specific heat exhibits a second broad maximum around $T \approx 0.67|J_1|$. Such a double-peak structure in the specific heat has already been observed for $J_2 = -0.3J_1$ on a finite lattice with $N = 16$ sites,²¹ and by TMRG at $J_2 = -0.4J_1$.⁶ Note that the results for C of Ref. 6 are restricted to temperatures $T \geq 0.013|J_1|$ in this parameter regime, and the TMRG method might be plagued by convergence problems at low temperatures. Despite the finite-size effects in our data at low temperatures we can

clearly resolve the low-temperature peak in C (see inset of the middle panel of Fig. 2).

Our results for χ (top panel of Fig. 2) differ qualitatively from those obtained for $J_2 = -0.3J_1$ and $N=16$ in Ref. 21 by ED. In particular, we find a singlet ground state for all periodic systems with $|J_1| < 4J_2$ investigated, in contrast to Ref. 21. However, we do find good agreement with the more recent TMRG results for χ .⁶

It is not entirely trivial to separate the low- and high-temperature features in C and χ into FM and AFM ones. Let us compare the case $J_2 = -J_1/3$ with an unfrustrated FM chain (Fig. 2 includes results for $J_2=0$, $J_1 < 0$, and $N=20$). In both cases, there is a broad maximum in C at high temperatures, although numerical values are different. Concerning the low-temperature peaks in χ and C , note that, for $J_1 = -3J_2$, the FM $s=N/2$ multiplet is located at an energy of about $N|J_1|/40$ above the $s=0$ ground state. Since this energy scale roughly agrees with the temperature scale of the low-temperature maxima, it is conceivable that they correspond to FM fluctuations above an AFM ground state.

Finally, we note that the entropy of the frustrated FM chain ($J_2 = -J_1/3$) is larger than that of the simple FM chain ($J_2=0$) over a wide temperature range (see bottom panel of Fig. 2). Only for very low temperatures does the FM ground state lead to a bigger entropy for $J_2=0$.

To summarize, we have studied the ground-state phase diagram of a frustrated FM chain in a magnetic field and found an EO phase characterized by bound pairs of magnons. The boundary of this phase appears to be first order and terminates for $h \rightarrow h_{\text{sat}}$ at $J_2 \approx -0.38J_1$.¹² At larger FM

$|J_1|$, changes in the step height of the magnetization curves signal the presence of further phases, which need to be studied in more detail. It would also be desirable to better understand the low-lying excitations in the different phases and to compare to the case of the frustrated antiferromagnetic chain.³ Our phase diagram differs substantially from recent mean-field predictions.⁹ In particular, our DMRG data exhibit a smooth transition to saturation for any $J_1 > -4J_2$, in contrast to previous studies.^{9,18} This observation may also be relevant for the transition to saturation in the frustrated square lattice ferromagnet.²² The parameters relevant to LiCuVO_4 (Ref. 5) lie well inside the EO phase where the theoretical magnetization curves are completely smooth.

Furthermore, we have discussed thermodynamic properties.¹⁰ The most prominent feature for $J_2 = -J_1/3$, $h=0$ is a double-peak structure in the specific heat.^{6,21} The excitation spectrum is not reflected directly in thermodynamic quantities, but microscopic probes such as neutron scattering or nuclear magnetic resonance should be able to differentiate between gapped $\Delta S^z=1$ excitations and gapless $\Delta S^z=2$ excitations.

We are grateful for generous allocation of CPU time on compute-servers at the Rechenzentrum of the TU Braunschweig (COMPAQ ES45, IBM p575) and the HLRN Hannover (IBM p690) as well as the technical support of J. Schüle. We thank M. Banks, D. C. Cabra, S. Kancharla, R. Kremer, R. Melko, and H.-J. Mikeska for fruitful discussions and valuable comments on the manuscript. This work was supported in part by the NSF Grant No. DMR-0443144.

¹U. Schollwöck, J. Richter, D. J. J. Farnell, and R. F. Bishop, *Quantum Magnetism*, Lecture Notes in Physics Vol. 645 (Springer-Verlag, Berlin, 2004); H. T. Diep, *Frustrated Spin Systems* (World Scientific, Singapore, 2005).

²H.-J. Mikeska and A. K. Kolezhuk, in *Quantum Magnetism*, edited by U. Schollwöck *et al.*, Lecture Notes in Physics Vol. 645 (Springer-Verlag, Berlin, 2004), p. 1.

³K. Okunishi and T. Tonegawa, J. Phys. Soc. Jpn. **72**, 479 (2003); Phys. Rev. B **68**, 224422 (2003).

⁴M. Hase, H. Kuroe, K. Ozawa, O. Suzuki, H. Kitazawa, G. Kido, and T. Sekine, Phys. Rev. B **70**, 104426 (2004).

⁵M. Enderle, C. Mukherjee, B. Fåk, R. K. Kremer, J.-M. Broto, H. Rosner, S.-L. Drechsler, J. Richter, J. Malek, A. Prokofiev, W. Assmus, S. Pujol, J.-L. Raggazzoni, H. Rakoto, M. Rheinstädter, and H. M. Rønnow, Europhys. Lett. **70**, 237 (2005).

⁶H. T. Lu, Y. J. Wang, Shaojin Qin, and T. Xiang, cond-mat/0603519 (unpublished).

⁷S. R. White, Phys. Rev. Lett. **69**, 2863 (1992); Phys. Rev. B **48**, 10345 (1993).

⁸T. Hamada, J. Kane, S. Nakagawa, and Y. Natsume, J. Phys. Soc. Jpn. **57**, 1891 (1988).

⁹D. V. Dmitriev and V. Y. Krivnov, Phys. Rev. B **73**, 024402 (2006).

¹⁰Thermodynamic quantities have been computed in the region $-4 \leq J_1/J_2 \leq 4$ for rings with $N=16, 20$. They are available for download at www.theorie.physik.uni-goettingen.de/~honecker/j1j2-td/ at $h=0$ on a grid in the J_1/J_2 - T/J_2 plane. Results with an external magnetic field can be provided upon request.

¹¹M. Banks *et al.* (unpublished).

¹²A. V. Chubukov, Phys. Rev. B **44**, 4693 (1991).

¹³D. C. Cabra, A. Honecker, and P. Pujol, Eur. Phys. J. B **13**, 55 (2000).

¹⁴A. Luther and I. Peschel, Phys. Rev. B **12**, 3908 (1975).

¹⁵N. M. Bogoliubov, A. G. Izergin, and V. E. Korepin, Nucl. Phys. B **275**, 687 (1986).

¹⁶S. Qin, M. Fabrizio, L. Yu, M. Oshikawa, and I. Affleck, Phys. Rev. B **56**, 9766 (1997); D. C. Cabra, A. Honecker, and P. Pujol, Phys. Rev. B **58**, 6241 (1998).

¹⁷A. A. Nersisyan and A. M. Tsvelik, Phys. Rev. Lett. **78**, 3939 (1997).

¹⁸A. A. Aligia, Phys. Rev. B **63**, 014402 (2001).

¹⁹A. Kolezhuk and T. Vekua, Phys. Rev. B **72**, 094424 (2005).

²⁰M. E. Zhitomirsky and A. Honecker, J. Stat. Mech.: Theory Exp. P07012 (2004).

²¹S. Thanos and P. Moustanis, Physica A **271**, 418 (1999).

²²N. Shannon, T. Momoi, and P. Sindzingre, Phys. Rev. Lett. **96**, 027213 (2006).